

Clinically-Relevant Rapamycin Treatment Regimens Enhance CD8⁺ Effector Memory T Cell Function In The Skin and Allow their Infiltration into Cutaneous Squamous Cell Carcinoma

Ji-Won Jung, Margaret Veitch, Jennifer A. Bridge, Nana H. Overgaard, Jazmina L. Cruz, Richard Linedale, Michael E. Franklin, Nicholas A. Saunders, Fiona Simpson, Ian H. Frazer, Raymond J. Steptoe & James W. Wells

To cite this article: Ji-Won Jung, Margaret Veitch, Jennifer A. Bridge, Nana H. Overgaard, Jazmina L. Cruz, Richard Linedale, Michael E. Franklin, Nicholas A. Saunders, Fiona Simpson, Ian H. Frazer, Raymond J. Steptoe & James W. Wells (2018): Clinically-Relevant Rapamycin Treatment Regimens Enhance CD8⁺ Effector Memory T Cell Function In The Skin and Allow their Infiltration into Cutaneous Squamous Cell Carcinoma, Oncoimmunology

To link to this article: <https://doi.org/10.1080/2162402X.2018.1479627>



View supplementary material [↗](#)



Published online: 30 Jul 2018.



Submit your article to this journal [↗](#)



View Crossmark data [↗](#)

ORIGINAL RESEARCH



Clinically-Relevant Rapamycin Treatment Regimens Enhance CD8⁺ Effector Memory T Cell Function In The Skin and Allow their Infiltration into Cutaneous Squamous Cell Carcinoma

Ji-Won Jung^{a*}, Margaret Veitch^{a*}, Jennifer A. Bridge^a, Nana H. Overgaard ^{a,b}, Jazmina L. Cruz^a, Richard Linedale^a, Michael E. Franklin^c, Nicholas A. Saunders^a, Fiona Simpson ^a, Ian H. Frazer^a, Raymond J. Steptoe^a, and James W. Wells ^a

^aThe University of Queensland Diamantina Institute, Translational Research Institute, Brisbane, QLD Australia; ^bDivision of Immunology & Vaccinology, National Veterinary Institute, Technical University of Denmark, Lyngby, Denmark; ^cDepartment of Clinical Pharmacology, Princess Alexandra Hospital, Queensland Health, Brisbane, QLD, Australia

ABSTRACT

Patients receiving immunosuppressive drugs to prevent organ transplant rejection exhibit a greatly increased risk of developing cutaneous squamous cell carcinoma (SCC). However, not all immunosuppressive drugs confer the same risk. Randomised, controlled trials demonstrate that switching renal transplant recipients receiving calcineurin inhibitor-based therapies to mammalian target of rapamycin (mTOR) inhibitors results in a reduced incidence of *de novo* SCC formation, and can even result in the regression of pre-existing premalignant lesions. However, the contribution played by residual immune function in this setting is unclear. We examined the hypotheses that mTOR inhibitors promote the enhanced differentiation and function of CD8⁺ memory T cells in the skin. Here, we demonstrate that the long-term oral administration of rapamycin to achieve clinically-relevant whole blood drug target thresholds, creates a “low rapamycin dose” environment in the skin. While both rapamycin and the calcineurin inhibitor tacrolimus elongated the survival of OVA-expressing skin grafts, and inhibited short-term antigen-specific CD8⁺ T cell responses, rapamycin but not tacrolimus permitted the statistically significant infiltration of CD8⁺ effector memory T cells into UV-induced SCC lesions. Furthermore, rapamycin uniquely enhanced the number and function of CD8⁺ effector and central memory T cells in a model of long-term contact hypersensitivity provided that rapamycin was present during the antigen sensitization phase. Thus, our findings suggest that patients switched to mTOR inhibitor regimens likely experience enhanced CD8⁺ memory T cell function to new antigen-challenges in their skin, which could contribute to their lower risk of *de novo* SCC formation and regression of pre-existing premalignant lesions.

ARTICLE HISTORY

Received 20 October 2017
Revised 15 May 2018
Accepted 16 May 2018

KEYWORDS


T cells; memory; skin; transplantation


Introduction

Renal transplant recipients often receive triple therapy with combinations of Glucocorticoids (prednisolone or prednisone), calcineurin inhibitors (cyclosporine or tacrolimus) and anti-proliferative agents (azathioprine or mycophenolic acid) to prevent rejection of their allografts.^{1,2} Worldwide, these patients suffer a 65–250 fold increased risk of non-melanoma skin cancer (NMSC; primarily basal cell carcinoma and squamous cell carcinoma, SCC) development compared with the general population.^{3,4} A single follow-up study of renal transplant recipients in Queensland reported increased NMSC incidence with increasing duration of immunosuppression, with over 50% developing at least one tumour within 10 years of starting immunosuppressive therapy.³ Some renal transplant patients currently presenting to the Princess Alexandra Hospital, Brisbane, Australia require the removal of ~120 primary skin tumors each year. Metastatic SCC,

and not organ failure or rejection, is now the leading cause of death in renal transplant patients in Australia.⁵

Despite receiving triple therapy, the substitution of a single agent (i.e. a calcineurin inhibitor for a mTOR inhibitor) has been shown to reduce *de novo* SCC formation,^{6–9} induce regression of pre-existing premalignant lesions,⁸ and in at least 3 separate clinical studies lead to 100% tumour regression of cutaneous Kaposi's sarcoma lesions in kidney transplant recipients, with no apparent loss of graft function.^{10–12} However, conversion from calcineurin inhibitors to mTOR inhibitors is frequently associated with a significant increase in adverse events, including oedema, diarrhoea, headache, mouth ulceration, pneumonitis, and impaired wound healing that ultimately combine to result in a high degree of drug discontinuation.^{6–8,13–15} Nevertheless, there is substantial benefit associated with conversion to mTOR inhibitors in terms of the anti-neoplastic effect on SCC.

CONTACT James W. Wells  j.wells3@uq.edu.au  The University of Queensland Diamantina Institute, Translational Research Institute, 37 Kent Street, Woolloongabba QLD 4102, Australia

 Supplemental data for this article can be accessed on the publisher's website.

*These authors contributed equally to this work

Color versions of one or more of the figures in the article can be found online at www.tandfonline.com/koni.

The direct effects of calcineurin inhibitors and mTOR inhibitors on tumour growth and survival have been extensively studied in the laboratory, with a general consensus that calcineurin inhibitors are pro-neoplastic while mTOR inhibitors are anti-neoplastic.¹ However, patients treated topically with the calcineurin inhibitor tacrolimus for moderate to severe atopic dermatitis do not display an increased risk of SCC formation.^{16–18} This argues against a pro-neoplastic effect of calcineurin inhibitors in the skin solely due to direct transformation events. Similarly, at least 2 independent clinical studies have reported that the use of high doses of the mTOR inhibitor sirolimus (also known as rapamycin) abolish the anti-tumour effects shown by low doses of sirolimus, leading to Kaposi sarcoma development and/or recurrence.^{19,20} Recently, the long-term administration of the mTOR inhibitor everolimus to patients was shown to correlate with an increase in the production of Eomesodermin⁺ memory CD8⁺ T-cells.²¹ These observations cast doubt on the assumption that the anti-neoplastic effects of mTOR inhibitors rest solely on direct tumour growth inhibition. Together, these studies may suggest a role for residual immune function in the differential effects of calcineurin inhibitors and mTOR inhibitors on SCC growth and survival. The effects that these inhibitors have on the function of immune cells within SCC however, remain largely unstudied.

In mice, treatment with low doses (75 µg/kg; blood levels; 5–20 ng/ml) of the mTOR inhibitor rapamycin following acute lymphocytic choriomeningitis virus infection was described to enhance not only the quantity but also the quality of virus-specific memory CD8⁺ T cells.²² Mechanistically, low dose rapamycin treatment increased the number of memory precursor cells during the T cell expansion phase, which resulted in an accelerated memory T cell differentiation program (effector to memory transition) during the T cell contraction phase.²² These effects were not seen when high doses (600 µg/kg; blood levels; 40–100 ng/ml) of rapamycin were used when, conversely, T cell responses during the expansion phase were inhibited. The impact of low dose rapamycin may be linked to the importance of cellular metabolism in determining T cell differentiation; a pathway heavily regulated by mTOR.²³ mTOR inhibition facilitates the transition of highly metabolic effector cells into a more catabolic state required for memory cell differentiation in response to mitogenic and growth factor withdrawal.²⁴ mTOR inhibition, but not calcineurin inhibition, has been shown to produce memory CD8⁺ T cell precursors that demonstrate enhanced subsistence and antigen-recall responses upon adoptive transfer.²⁵ Importantly, low dose mTOR inhibition produces little interference with effector molecules such as IFN-γ, perforin, or granzyme B, leading to the suggestion that anti-tumour T cell responses might be permitted in patients treated with mTOR inhibitors.²⁶

We recently examined the abundance of multiple T cell subsets in the skin of kidney transplant patients receiving either rapamycin (sirolimus)- or calcineurin inhibitor-based drug therapy, and demonstrated that sirolimus treatment, but not calcineurin inhibitor treatment, led to significant increases in the abundance of CD8⁺ memory T cells in sun-exposed skin as compared to non-sun exposed skin in inpatient

analyses.²⁷ CD8⁺ T cells play a critical protective role in the body by recognizing and destroying virally-infected- and malignant cells,^{28–33} and by influencing other immune cell populations through the production of Th1-biased cytokines including IFN-γ.^{34,35} We have shown previously that SCC lesions specifically display a lower abundance of CD8⁺ T cells than premalignant lesions in immune-competent patients.³⁶ Given this link between mTOR inhibitor use and CD8⁺ memory T cell abundance in patient skin, we examined the role of clinically-relevant rapamycin concentrations in the differentiation and function of CD8⁺ memory T cells in SCC and the skin.

Materials and methods

Mice

All animal procedures were approved by the University of Queensland Animal Ethics Committee; Approval Numbers 342/11 and 466/14. C57BL/6J mice were purchased from the Animal Resources Facility Perth, Australia. K5mOVA mice, which express membrane-bound OVA in the skin under the control of the K5 promoter,³⁷ K14 HPV38 E6/E7 mice, which express the E6 and E7 genes of Human Papillomavirus (HPV) type 38 under the control of the Keratin 14 promoter,³⁸ OT-II mice, and B6.SJL (CD45.1⁺) x OT-I, and Nzeg (GFP⁺) x OT-I mice carrying a MHC class I-restricted transgenic TCR for the OVA_{257–264} (SIINFEKL) peptide were bred and maintained locally at the Translational Research Institute Biological Research Facility (Brisbane, Australia). All mice used were 6–12 wk females and were housed under specific pathogen-free conditions.

Antibodies and reagents

OVA_{257–264} (SIINFEKL) peptide was purchased from Proimmune Ltd (Oxford, UK). Ovalbumin (OVA), bovine serum albumin (BSA), phytohemagglutinin (PHA), zinc sulphate, saponin and 2,4-dinitrofluorobenzene (DNFB) were purchased from Sigma-Aldrich (St. Louis, MO). Acetonitrile, Titrisol buffer, and tert-butyl methyl ether (TBME) were purchased from Merck KGaA (Darmstadt, Germany). Tacrolimus and rapamycin were purchased from LC Laboratories (Woburn, MA). Flow-Count Fluorospheres were purchased from Beckman Coulter (Miami, FL, USA) and carboxyfluorescein diacetate succinimidyl ester (CFSE), CellTrace Violet (CTV), Live/Dead Fixable Aqua Dead Cell Stain, and anti-CD3/CD28 Dynabeads were purchased from Thermo Fisher Scientific (Waltham, MA, USA). Purified 53–5.8 (anti-CD8β-depleting antibody) and anti-HRPN isotype control was purchased from BioXCell (West Lebanon, NH, USA). Brefeldin A, FITC-conjugated H57-597 (anti-TCRβ), APC-conjugated 53–6.7 (anti-CD8α), 53–5.8 (anti-CD8β.2), XMG1.2 (anti-IFN-γ), 145-2C11 (anti-CD3ε), and H1.2F3 (anti-CD69), PE-conjugated MEL-14 (anti-CD62L), B20.1 (anti-TCRVα2), and 4C7 (anti-CD207), PE/Dazzle-conjugated 16-10A1 (anti-CD80), AX647-conjugated MF-14 (anti-FoxP3), AX488-conjugated HM40-3 (anti-CD40), PE-Cy7-conjugated RI7217 (anti-CD71), A20 (anti-CD45.1), GK1.5 (anti-CD4), N418 (anti-CD11c), H1.2F3 (anti-CD69) and 53–6.7 (anti-CD8α), PerCP-Cy5.5-conjugated 104 (anti-CD45.2) and 145-2C11 (anti-CD3ε) and H57-597 (anti-TCRβ), APC-Cy7-conjugated IM7 (anti-CD44) and

M5/114.15.2 (anti-I-A/I-E), BV605-conjugated 53–6.7 (anti-CD8 α), BV650-conjugated M1/70 (anti-CD11b), BV785-conjugated MP6-XT22 (anti-TNF α) and GL-1 (anti-CD86), and BV421-conjugated 2E7 (anti-CD103) were purchased from Biolegend (San Diego, CA, USA) or eBioscience (San Diego, CA, USA). Collagenase D, Dispase II, and DNase 1 were purchased from Roche (Indianapolis, IN, USA). Ascomycin – the internal standard for tacrolimus – was supplied by Fujisawa Pharmaceutical Company (Osaka, Japan). 32-O-desmethoxyrapamycin – the internal standard for rapamycin – was supplied by Wyeth-Ayerst Research (Princeton, NJ, USA).

Dendritic cell isolation from skin

Ears and inguinal lymph nodes were harvested from mice recipient of control or drug diets for 22 days. On the day prior to harvest the mice received an injection containing 25 μ g of CpG and 25 μ g of Poly I:C s.c. near the inguinal lymph nodes. Ears were split into dorsal and ventral halves using forceps and excess collagen removed by scraping with a sharp blade. Ear halves were then placed dermis-side down in RPMI media containing 2.5mg/ml Dispase II for 60 minutes at 37°C to allow separation of epidermal sheets using forceps. Epidermal and dermal tissue was placed into separate tubes, cut into small fragments, and digested for 45 minutes (epidermis) or 60 minutes (dermis) at 37°C with 1 mg/ml collagenase D and 20 μ g/ml Dnase 1. Tissues were then passed through a 70 μ m cell strainer (BD Biosciences, San Jose, CA) to create a single-cell suspension.

T cell isolation from skin and AK/SCC lesions

To release cells from ear skin, back skin, and AK/SCC lesions for analysis by flow cytometry, harvested tissue was cut into small fragments and digested for 1 hour at 37°C with 1 mg/ml collagenase D and 20 μ g/ml Dnase 1. Tissues were then passed through a 70 μ m cell strainer (BD Biosciences, San Jose, CA) to create a single-cell suspension.

Phenotypic and functional analysis of cell populations by flow cytometry

Isolated cells were resuspended in PBS/0.5% FBS and incubated with Fc-block and 2% rat serum for 20 minutes on ice to block non-specific antibody staining. Intracellular staining for Foxp3 and CD207 (lymph nodes and dermis only) was performed using the Foxp3/Transcription Factor Staining Buffer Set Kit (eBioscience) according to the manufacturers' instructions. Monoclonal antibodies for surface staining were subsequently added for 30 minutes on ice in concert with Live/Dead Aqua Stain to elucidate live cell populations. Immediately before FACS acquisition, Flow-Count Fluorospheres were added to allow assessment of total cell counts. For analysis of intracellular cytokine production, bone marrow-derived dendritic cells (generated as described previously using IL-4 and GM-CSF³⁹ (cytokines from R&D Systems, Minneapolis, MN) were pulsed with 100 μ g/ml OVA or BSA protein for 4 hours, and then 10,000 cells were co-cultured with each ear homogenate sample for 16.5 hours at 37°C. 5 μ g/ml Brefeldin A was added for the last 4.5 hours of culture, and intracellular staining performed as described previously.⁴⁰ LSR II, FACSCanto, or LSR Fontessa (BD

Biosciences, San Jose, CA) Flow Cytometers were used for FACS analysis, and Kaluza (Beckman Coulter, Orange County, CA) and FlowJo (TreeStar Inc., Ashland, OR) softwares were used for data analysis.

Diet-based drug delivery

All customised mice diet was manufactured by Specialty Feeds (Perth, WA). Briefly, tacrolimus or rapamycin was mixed with caster sugar and then incorporated into standard mouse diet. 1.5 g of tacrolimus or 1.0 g of rapamycin was mixed with 100 g of caster sugar and 9.9 kg of standard mouse diet to result in tacrolimus-diet or rapamycin-diet respectively. Food colouring was added to distinguish drug types. During the manufacturing process the pellets were air-dried overnight rather than dried in an oven in order to minimise the amount of heat applied. The final product was sealed in airtight bags and stored at 4°C protected from light to ensure minimal degradation. Pellet volumes in feed hoppers were kept to a minimum and restocked every 3–4 days for the duration of the experiments.

Quantification of drug concentrations in blood and tissues

Blood. Blood was collected in EDTA, immediately mixed to prevent coagulation, and stored at –20°C. For consistency, samples were collected at the same time each day (12 noon). 25 μ l of the blood samples were transferred into a 96-well round bottom 2 ml polypropylene deep well plate (Axygen Scientific, Union City, CA). After addition of 100 μ l 0.1 M zinc sulphate into each well, the plate was vortexed for 10 secs. 250 μ l of HPLC-grade acetonitrile containing 5 μ g/L internal standard (ascomycin or 32-O-desmethoxyrapamycin) was added per well, vortexed for 2 mins, and centrifuged for 3 mins at 800g. 20 – 40 μ l of the supernatant was then analysed using LC-MS/MS (Alliance HT LC system interfaced to a Quattro Micro tandem mass spectrometer (Waters Corporation, Milford, MA) or Quattro-Premier mass spectrometer (Waters Corporation) was used for measurements of tacrolimus or rapamycin respectively. Calibration standards and quality control samples were prepared in human blood using independent stock drug solutions. The mass transitions monitored for tacrolimus were m/z 821.3 \rightarrow 768.3 and m/z 809.3 \rightarrow 756.3 for the internal standard (ascomycin), with a dwell time of 150 ms, and the mass transitions monitored for rapamycin were m/z 931.3 \rightarrow 864.2 and m/z 901.3 \rightarrow 834.2 for the internal standard (32-O-desmethoxyrapamycin), with a dwell time of 100 ms.

Skin. 4 cm² of skin/mouse was carefully excised and subcutaneous tissues removed. Tissue samples were weighed, cut into small pieces, and then placed into a tissue grinding tube (Precellys[®] Lysing Kit; MK28-R; Bertin Technologies, Montigny-le-Bretonneux, France) containing 1 ml of Tritrisol buffer and 60 μ l of internal standard (ascomycin or 32-O-desmethoxyrapamycin). Rapamycin (0, 2, 5, 10, 50 ng/ml) and tacrolimus (0, 1, 5, 20, 50 ng/ml) standards were prepared in 50% methanol/MilliQ H₂O, and then diluted in Tritrisol buffer concentrate pH 10 to give a final concentration of 0, 0.2, 0.5, 1.0, 5.0 and 10.0 ng/ml for rapamycin and 0, 0.1, 0.5, 2.0 and 5.0 ng/ml for tacrolimus. Standard curves were prepared using skin of untreated mice and the addition of 1 ml of

reconstituted standards and 60 μ l of internal standard. Samples were homogenised using a Precellys[®] 24 Homogenizer (Bertin Technologies) at 6500 rpm, 30 seconds for 5 cycles, with the tubes placed on ice for at least 1 min between each cycle to prevent drug degradation. The homogenised contents were then transferred into 10 ml screw top glass tubes and 5ml of TBME added to each. The liquid-liquid extraction process was performed manually by inverting the tubes for at least 5 mins. Tubes were then centrifuged at room temperature at 1800g for 3 mins to separate all the layers, and the TBME containing the partitioned drug was transferred into a new 5 ml glass tube. The TBME was evaporated using a Sample Concentrator (Techne Dri-Block, DB-3D, Cambridge, England) at 35°C and the residue subsequently reconstituted with 200 μ l 50% methanol by vortexing thoroughly. Reconstituted samples were transferred into UPLC max recovery sample vials (Waters Corporation) and analysed using LC-MS/MS as described above.

Kidney. Drug quantification in the kidney was performed using the same protocol described in the skin assay. Kidneys were not perfused prior to harvest. Standards were prepared using drugs added to kidneys from untreated mice, to give a final concentration of 0, 2.0, 5.0, 10.0, 20.0 and 40.0 ng/ml for rapamycin and 0, 0.5, 2.0, 5.0, 10.0 and 20.0 ng/ml for tacrolimus.

Analysis of immunosuppression in vitro

Naïve splenocytes harvested from B6.SJL x OT-I mice were analysed for their ability to proliferate in the presence or absence of tacrolimus or rapamycin in response to co-culture with 0.1 μ g/ml SIINFEKL peptide, anti-CD3/CD28 beads (at a cells to beads ratio of 2:1) or 10 μ g/ml PHA. Cells were labelled with 2 μ M CFSE, plated in triplicate wells, and co-cultured with SIINFEKL, anti-CD3/CD28 beads, or PHA, with or without the indicated concentration of tacrolimus or rapamycin, for 72 hrs at 37°C. Cells were then stained with anti-CD8 β , and analysed by flow cytometry. The proliferation index (PI) was calculated as previously described.⁴¹

Analysis of immunosuppression in vivo

Splenocytes and lymph node cells were harvested from naive B6.SJL x OT-I, Nzeg x OT-I, or OT-II mice, labelled with 2 μ M CFSE or 5 μ M CTV, and intravenously injected (1×10^7 cells) into C57BL/6 recipient mice treated with either drug-incorporated diet or daily drug i.p. injection as indicated. OVA (50 μ g) or BSA (50 μ g) was injected s.c. near both inguinal lymph nodes on Day 3. Inguinal lymph nodes were harvested on Day 6, stained with the relevant antibodies, and analysed via flow cytometry.

UV-induction of SCC

The backs of K14 HPV38 E6/E7 mice were shaved and exposed to UV light 3 times per week using UV bulbs purchased from Vilber Lourmat (model T-40M, 40 Watts, Marne La Vellee, France) and emitting peak UV irradiation in the UV-B spectrum (312 nm). Polyvinyl chloride (PVC) was used to filter out UVC light. The dose of UV started at 120 mJ/cm² on Week 1, and was gradually increased to 450 mJ/cm² by Week 20, and thereafter maintained at 450 mJ/cm² as

described previously.³⁸ CD8⁺ T cell subset identification and quantification was as described above.

Analysis of T cell function in the skin

Skin grafting. Ears were collected from donor C57BL/6 and K5m. OVA mice and separated into dorsal and ventral sides using forceps. Dorsal C57BL/6 (surgical control) and dorsal K5m. OVA (test) ear skin was then grafted side-by-side onto the thoracic flank region of an anesthetized C57BL/6 recipient. Grafts were held in place with antibiotic-permeated gauze (Bactigras; Smith and Nephew, London, U.K.) and bandaged with micropore tape (Micropore TM: 3M Health Care, Minnesota, U.S.) and an elastic bandage (3M Vetrap Bandaging TAPE, Vet n Pet Direct, Queensland, Australia). After 7 days, bandages were removed and grafts were photographed three times a week. For experiments examining CD8⁺ T cell depletion, mice were immunised with either 100 μ g of anti-CD8 β or 100 μ g of anti-HRPN isotype control i.p. on day 0, followed by 50 μ g injections on days 7, 10, and 35. For experiments examining the effect of drugs, mice were fed a drug-containing diet for 14 days before grafting and throughout the remainder of the experiment. Graft rejection was assessed by a loss of distinct border and signs of shrinkage, ulceration and/or necrosis to >80% of the graft area. Mice in which the control C57BL/6 graft did not heal were not included in final analyses.

Contact hypersensitivity (CHS). Mice were sensitized by a single s.c. injection into the flank skin containing 100 μ g OVA + 20 μ g saponin in 200 μ l of PBS (Day 0). Five days (short-term CHS response) or 45 (memory CHS response) days later, mice were challenged with OVA (15 μ g OVA in 10 μ l PBS, i.d.) in the right ear, and PBS (10 μ l PBS, i.d.) in the left ear. Ear thicknesses were measured after 24 and 48 hours using a dial thickness gauge (Peacock, Model G-1A; Ozaki, Tokyo, Japan), and the increase in ear swelling was determined as the percentage difference in ear thickness between the OVA-treated versus the PBS-treated ears of the same mouse. To achieve CD8⁺ T cell depletion, 10 μ g of anti-CD8 β antibody was injected i.p. on Days -7, -4, -1, and 3 (short-term CHS), or on Days 33, 36, 39, and 43 (memory CHS). CD8⁺ T cell depletion in the blood was assessed on Day 0 (short-term CHS), or on Day 40 (memory CHS), by FACS analysis, and was found to consistently result in at least 99.7% reduction in total CD8⁺ T cell numbers. CD8⁺ T cell numbers in the ear skin were determined as described above 8 days following antigen challenge when ear swelling was judged to have completely subsided.

Statistical analysis

All statistical analysis was carried out using GraphPad Prism version 6.02 or 7.03 (GraphPad Software, San Diego, CA, USA). Statistical tests are as indicated in figure legends. A *P* value of *p* < 0.05 (*) was considered significant. *p* < 0.01 (**), *p* < 0.001 (***), and *p* < 0.0001 (****) are indicated.

Results

Establishment of drug diets to deliver clinically-relevant in vivo drug concentration profiles

Immunosuppressant drugs are administered orally to transplant patients ensuring consistent and predictable long-term drug delivery. In order to deliver rapamycin or tacrolimus

orally to mice over prolonged time-periods, we established customised drug-incorporated mouse diets. Before the incorporation of the drugs into the diets we confirmed the ability of rapamycin and tacrolimus to suppress CD8⁺ T cell proliferation *in vitro*. Splenocytes from OT-I transgenic mice were labelled with CFSE and stimulated in the presence or absence of rapamycin (Supplementary Figure 1A) or tacrolimus (Supplementary Figure 1B). SIINFEKL peptide, anti-CD3/CD28 beads, or phytohemagglutinin (PHA) were used to assess CD8⁺ T cell proliferation in response to antigen-specific stimulation, TCR/co-stimulatory-dependent stimulation, or mitogen-stimulation respectively. The Proliferation Index of CD8⁺ T cells was calculated based on CFSE-dilution⁴¹ and observed to be significantly reduced when cells were treated with rapamycin or tacrolimus in all stimulation conditions.

Rapamycin or tacrolimus was then incorporated into standard mouse diet, which was stored in vacuum-sealed bags in the dark at 4°C in order to counteract the loss of drug with time and ensure predictable drug-delivery. To confirm that clinically-relevant drug thresholds were being established following the administration of customised drug-diets, LC-MS/MS analysis was performed on unfractionated whole mouse blood over time. As shown in Supplementary Figure 1C, mice fed the rapamycin-diet eventually established a plateau blood concentration between 15- and 22 ng/ml, which is within the clinical target range (10 – 30 ng/ml).⁴² Mice fed tacrolimus-diet achieved blood concentrations of tacrolimus between 3 – and 9 ng/ml, which is on the lower end of the clinical target range (5 – 20 ng/ml)⁴³ (Supplementary Figure 1D), however we chose not to increase the dose of tacrolimus due to an associated increase in complications following experiments involving surgical skin-grafting procedures. Mice were weighed each week and were found to demonstrate a slight reduction in weight gain when compared with mice fed a control diet (Supplementary Figure 1E), but were otherwise healthy and active. The customised drug diets therefore, provided a means to deliver rapamycin and tacrolimus to mice in a physiologically relevant manner and maintain clinically-relevant drug concentrations in the blood over a prolonged period of time.

Clinically-relevant rapamycin concentrations have little impact on the abundance of epidermal and dermal dendritic cells, or the abundance of CD8⁺ T cells in the skin draining lymph nodes

To examine the consequence of clinically-relevant concentrations of rapamycin on immune cell abundance in the skin and skin-draining lymph nodes, we analysed dendritic cell (DC) subsets in the epidermis and dermis, and DC and T cell subsets in the skin draining lymph nodes. In the epidermis, numbers of CD207⁺(Langerin⁺)MHC-II⁺CD11c⁺ Langerhans cells (LCs) were not significantly altered by rapamycin-diet or tacrolimus-diet compared with the control (No Drug) group (Figure 1A). In the dermis, the frequencies of DC subsets, including Langerin⁺CD103⁺ dermal DC (dDC) and Langerin⁺CD103⁻ transmigrating LCs, also appeared unaffected by either drug diet (Figure 1B). To determine the frequency of DC and T cells subsets in the skin-draining lymph nodes, we mechanically disrupted pairs of inguinal lymph nodes and performed FACS analyses of single cell

suspensions. As shown in (Figure 1C), neither rapamycin nor tacrolimus had a significant impact on the abundance of MHC-II⁺CD11c⁺CD8α⁺ lymph node-resident DC. Tacrolimus but not rapamycin however, reduced the absolute number of MHC-II⁺CD11c⁺CD11b⁺ lymph node-resident DC. Rapamycin, by contrast, slightly increased the proportion of CD11b⁺ DC within the MHC-II⁺CD11c⁺ DC compartment. Interestingly, while neither rapamycin nor tacrolimus significantly reduced the number of CD8α⁻CD11b⁻ Langerin⁺CD103⁺ dDC or CD8α⁻CD11b⁻ Langerin⁺CD103⁻ transmigrating LCs, both drugs reduced the number of CD103⁺CD207⁻ DC (Figure 1D). To examine the impact of clinically-relevant rapamycin concentrations on the activation of lymph node DC, we injected CpG/Poly I:C s.c near the inguinal lymph nodes 24 hours before lymph node harvest, however no significant differences in the expression of CD86, CD80, or CD40 activation markers by lymph node DC subsets were detected between drug-treated and control groups (data not shown).

Overall, and in contrast to tacrolimus-diet, rapamycin-diet did not lead to a significant reduction in the total number of cells or the number of CD8⁺ T cells in the skin-draining lymph nodes (Figure 1E). Both rapamycin-diet and tacrolimus-diet however, led to a reduction in the absolute number of CD4⁺ T cells and FoxP3⁺CD4⁺ regulatory T cells within the skin-draining lymph nodes (Figure 1E), although the effects of tacrolimus-diet were more pronounced. Tacrolimus-diet, but not rapamycin-diet, also reduced the proportion of FoxP3⁺CD4⁺ regulatory T cells within the total CD4⁺ T cell pool (Figure 1E). Our attempts to similarly assess CD4⁺ T cell and FoxP3⁺CD4⁺ regulatory T cell abundance within the dermis were unsuccessful due to the cleavage of CD4 expression by dispase II treatment, which is needed to separate the epidermis from the dermis. Taken together, and with the exception of lymph node CD103⁺CD207⁻ DC, we observed that the abundance of CD8⁺ T cells in the skin-draining lymph nodes, and the abundance of DC subsets in the epidermis, dermis, and skin-draining lymph nodes, was similar when mice recipient of clinically-relevant concentrations of rapamycin were compared to control mice.

Clinically-relevant rapamycin concentrations induce CD8⁺ T cell suppression in the skin-draining lymph nodes

In order to assess whether clinically-relevant rapamycin concentrations attained functional CD8⁺ T cell suppression in the skin-draining lymph nodes, we introduced CFSE-labelled CD45.1⁺ OT-I lymphocytes into C57BL/6 recipient mice being treated with either drug-incorporated diet or daily i.p. drug injection. Three days later mice received Ovalbumin (OVA; 50 µg) or Bovine Serum Albumin (BSA; as a control; 50 µg) injected s.c. near the inguinal lymph nodes, and a further three days later the inguinal lymph nodes were harvested and analysed for CFSE-dilution in CD45.1⁺CD3e⁺CD8α⁺ cells by flow cytometry (see Supplementary Figure 2A for representative FACS plots). CD8⁺ T cell proliferation was found to be suppressed following the administration of rapamycin-diet to a level similar to that suppressed by the daily i.p. injection of 2mg/kg rapamycin (Figure 2A), similar to 600µg/kg rapamycin; Supplementary Figure 2B. Similarly, tacrolimus-diet suppressed CD8⁺ T cell

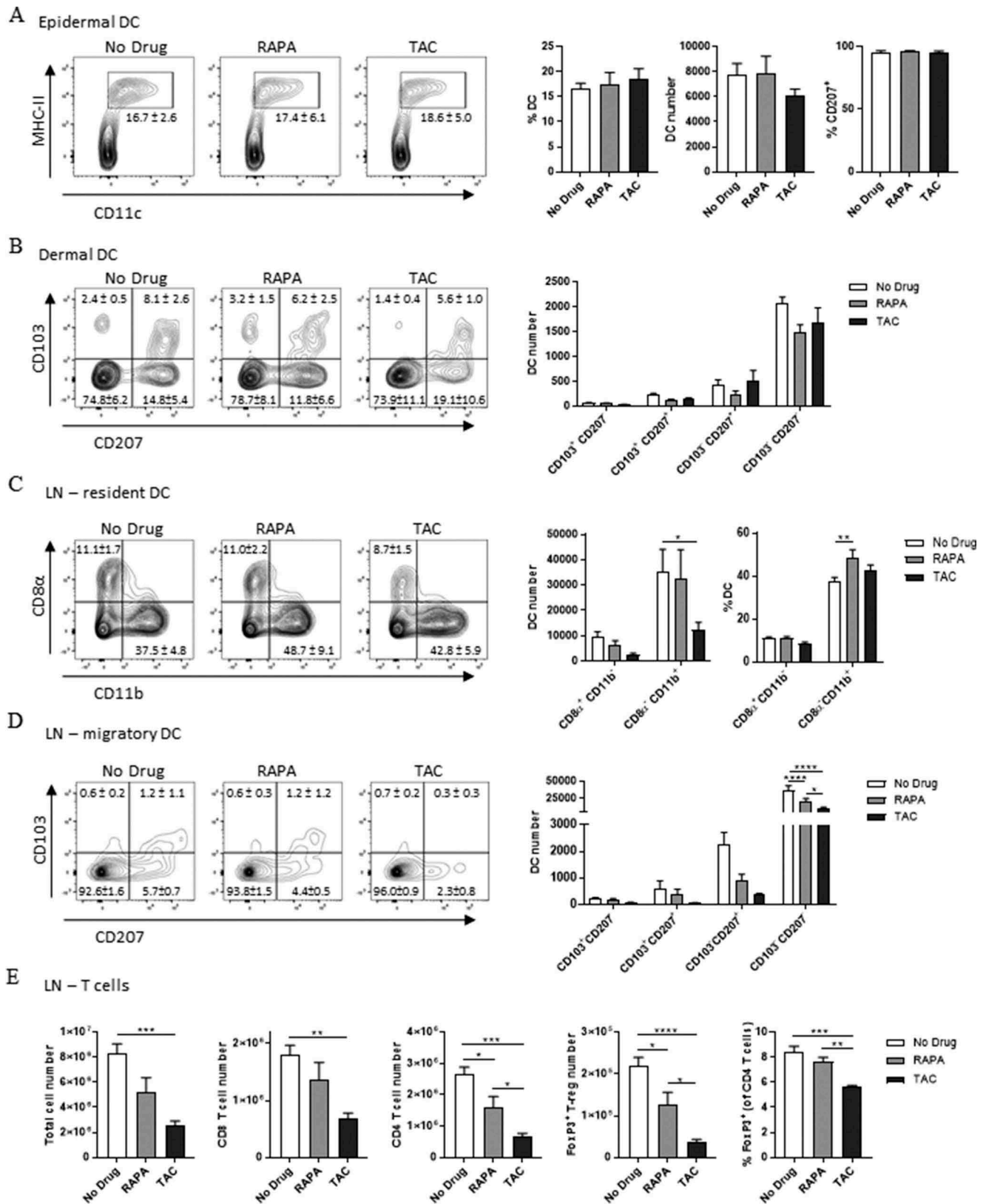


Figure 1. Clinically relevant doses of rapamycin do not impact DC numbers in the skin nor CD8⁺ T cell numbers in skin draining lymph nodes. (A-B) FACS analysis of DC in the epidermis (A) and dermis (B) of enzymatically digested ear skin from naïve mice (No Drug), or mice fed rapamycin-diet (RAPA) or tacrolimus-diet (TAC) for 22 days. Populations in plots are gated on Live CD45⁺ cells (A) and Live CD45⁺MHC II⁺CD11c⁺ cells (B). Numbers and percentages in bar graphs indicate mean absolute counts within analysed tissues or percentage of cells in the respective gate or quadrant ± SEM. (C-E) FACS analysis of DC (C-D) or Total/T cells (E) in pooled inguinal lymph node pairs from the same mice as A-B. Populations in plots are gated on Live MHC II⁺CD11c⁺ cells (C), Live MHC II⁺CD11c⁺CD8α⁺CD11b⁻ cells (D), and Live TCRβ⁺ cells ± CD8α, CD4, and/or FoxP3 (E). Numbers and percentages in bar graphs indicate mean absolute counts within paired inguinal lymph nodes or percentage of cells in the respective gate or quadrant ± SEM. Data were combined from 2 independent experiments with similar results. n = 6 mice/group. (A, B, and E) One-way ANOVA with post-hoc Tukey's multiple comparisons test. (C-D) Two-way ANOVA with post-hoc Tukey's multiple comparisons test.

proliferation to a level similar to that suppressed by the daily i.p. injection of 10mg/kg tacrolimus (Figure 2B). LC-MS/MS analysis of the blood taken the day before lymphocyte transfer showed that (at the time of sampling) the rapamycin-diet and rapamycin injections had established similar rapamycin concentrations in the blood (Figure 2C). However, a similar analysis of the two tacrolimus-delivery methods revealed that tacrolimus-diet had established higher tacrolimus concentrations in the blood than tacrolimus injection (Figure 2D). In contrast to the reduced proliferative capacity shown by CD8⁺ T cells in skin-draining lymph nodes, the proliferative capacity of CD4⁺ OT-II T cells did not appear to be significantly impacted by our rapamycin- and tacrolimus-diets (Figure 2E). Together, these data indicate that both rapamycin-diet and tacrolimus-diet induced systemic CD8⁺ T cell, but not CD4⁺ T cell, suppression *in vivo*.

Clinically-relevant rapamycin concentrations induce suppression of CD8⁺ T cell-mediated skin graft rejection.

Next, we examined the ability of rapamycin-diet and tacrolimus-diet to induce suppression of CD8⁺ T cell function in the skin using a skin graft rejection model. Transgenic skin engineered to express OVA under the K5 promoter (i.e. from K5mOVA mice) was rejected within ~30 days when grafted onto wild-type C57BL/6 recipient mice as determined by graft shrinkage and necrosis (Figure 3A; Isotype control). However, OVA-expressing skin was not rejected when recipient mice were depleted of CD8β⁺ T cells using a CD8β-depleting antibody (Figure 3A; αCD8β), thus highlighting the essential role played by CD8⁺ T cells in mediating skin graft rejection in this model. When recipient mice were treated before- and through-out the remainder of the experiment with either rapamycin-diet or tacrolimus-diet, approximately 50% of the skin grafts were not rejected (Figure 3B). In some experiments the drug diets were stopped on Day 109, resulting in the late-stage rejection of established skin grafts in approximately 50% (rapamycin-diet) to 80% (tacrolimus-diet) of cases (data not shown). The data indicate that the oral delivery of both rapamycin and tacrolimus can reduce CD8⁺ T cell-mediated skin graft rejection.

Rapamycin concentrations in the skin are low compared to the kidney

To examine the rapamycin and tacrolimus concentrations present in the blood, kidney, and skin as a consequence of rapamycin-diet and tacrolimus-diet respectively, we harvested blood, kidney, and skin after 20 days of drug diet and analysed drug concentrations by LC-MS/MS. As shown in Figure 4A-C, the concentration of rapamycin and tacrolimus was significantly higher at all three tissues sites when compared to non-drug treated controls, as expected. The concentration of rapamycin was significantly higher than tacrolimus in both the blood and kidney. Unexpectedly however, this situation was reversed in the skin, where the concentration of tacrolimus appeared significantly higher than rapamycin. Importantly, the levels of rapamycin in the skin were consistently around 5-15ng/gram, which might be considered to be in the “low” range when compared to previous reports reporting the memory T cell-promoting effects of low-dose rapamycin (blood levels; 5–20 ng/ml²²).

Rapamycin does not prevent CD8⁺ effector memory T cell infiltration into AK/SCC lesions in a model of uv-induced SCC formation

To explore the effects of rapamycin on CD8⁺ memory T cells within SCC lesions, we utilised a transgenic model in which the E6 and E7 genes of Human Papillomavirus (HPV) type 38 are expressed under the control of the Keratin 14 promoter.³⁸ K14 HPV38 E6/E7-transgenic mice develop premalignant actinic keratosis (AK)-like lesions and subsequently SCC following exposure to ultraviolet (UV) light 3 times per week over the course of 20+ weeks of UV-treatment (Figure 5A). As shown in (Figure 5A) (right panel), the emergence of tumors in this model appears as a “field effect” rather than as distinct pathologies, and therefore AK and SCC lesions are often interleaved and cannot be distinguished without histological assessment. Hence, we categorized harvested lesional skin as “AK/SCC”. We fed K14 HPV38 E6/E7 mice drug diets for the duration of UV-treatment and noted that rapamycin failed to significantly delay the emergence of AK/SCC lesions (Figure 5B). Unlike no drug control and tacrolimus-treated mice, rapamycin-treated mice did not display an increase in total CD8⁺ T cell abundance in AK/SCC lesions compared to fur-covered (UV-protected) normal skin (Figure 5C; fur-covered (UV-protected) normal skin = orange triangles, UV-exposed non-lesional skin = purple squares, and AK/SCC lesions = grey circles, as indicated by the colour-matched circles in (A)). However, rapamycin-treatment, but not tacrolimus treatment, allowed the increased infiltration of CD8⁺ effector memory T cells into AK/SCC lesions (Figure 5D). The abundance of CD8⁺ central memory T cells appeared unchanged regardless of treatment or tissue-type (Figure 5E), whereas CD8⁺ resident memory T cells appeared reduced when normal skin was compared to UV-exposed non-lesional skin (Figure 5F). Interestingly, this latter observation did not hold true when normal skin was compared to AK/SCC lesions, with the caveat that sample numbers are lower in rapamycin- and tacrolimus-treated lesional groups as some mice had to be harvested before the primary endpoint due to the emergence of adverse events (particularly skin ulceration and diarrhoea), in line with the long-term use of these drugs. These data demonstrate that rapamycin does not prevent CD8⁺ effector memory T cell infiltration into SCC lesions.

Rapamycin promotes central- and effector memory CD8⁺ T-cell differentiation and function in response to new antigen-challenges in the skin

Due to the known profoundly immunosuppressive effects of UV-treatment on effector and memory CD8⁺ T cell function and development,⁴⁴ it was not possible to make functional comparisons of CD8⁺ T cell populations in the skin of drug-treated mice using the K14 HPV38 E6/E7 model. Therefore, we examined memory CD8⁺ T cell function in drug-treated mice using skin contact hypersensitivity (CHS) responses (Figure 6A). In a short-term CHS model designed to look at acute CD8⁺ T cell function, drug diets were commenced on day -15 and maintained throughout the experiment. Mice were sensitized with OVA on day 0, and challenged with OVA in the ear skin on day 5 (Fig. 6Ai). 48 hours later both rapamycin and tacrolimus induced the suppression of skin swelling in response to antigen

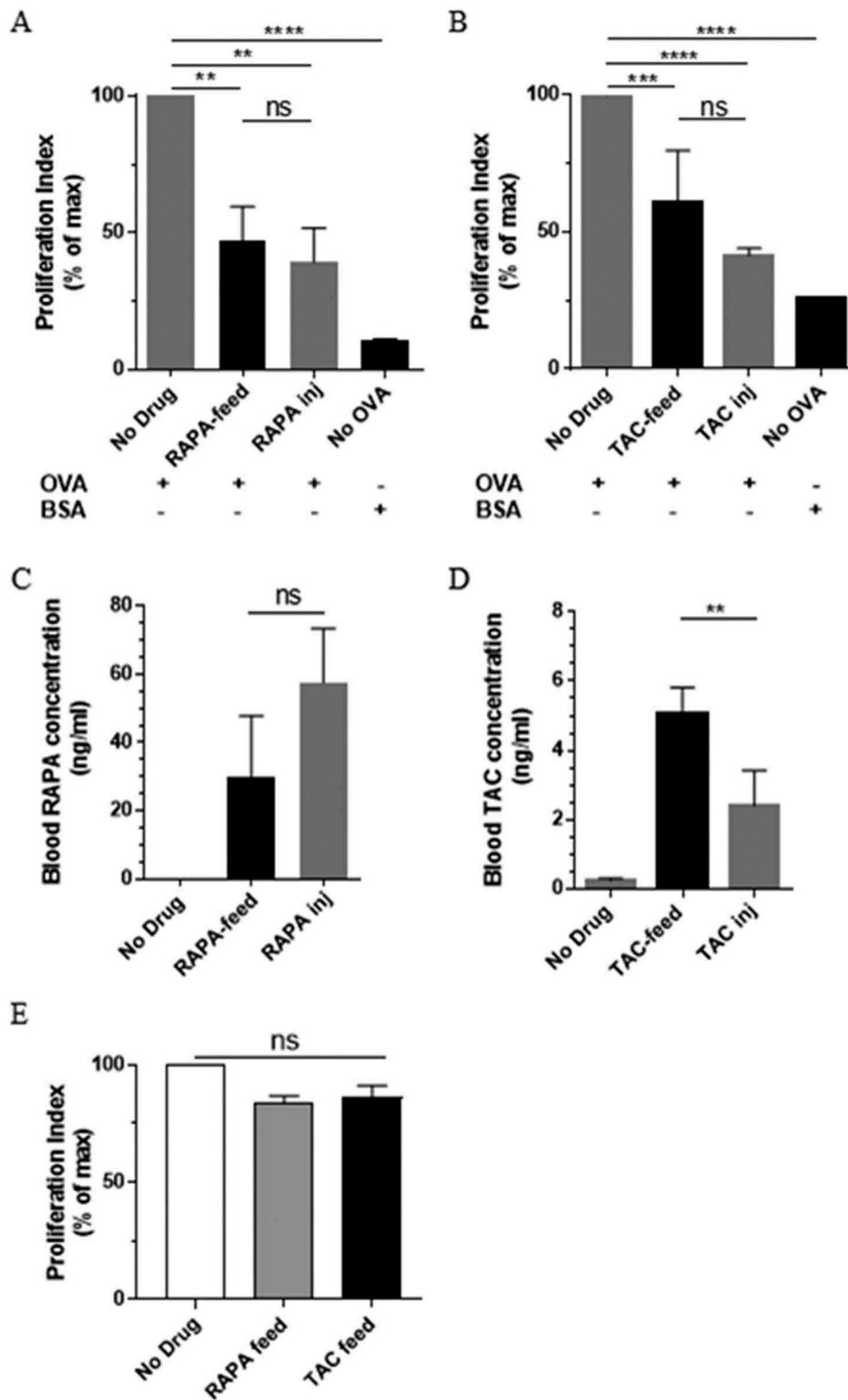


Figure 2. Drug diets lead to suppression of CD8⁺ T cell proliferation in skin-draining lymph nodes. CFSE-labelled CD45.1⁺ OT-I CD8⁺ T cells were adoptively transferred into C57BL/6 recipients pre-treated with either drug diet or daily drug injection. Treatments were maintained for the duration of the experiment. Inguinal lymph nodes were harvested 72 hours following the injection of OVA or BSA control protein into the skin, and assessed for CD45.1⁺ CD8⁺ T cell proliferation. (A) Rapamycin diet vs. daily injection. (B) Tacrolimus diet vs. daily injection. (C) and (D) Respective comparison of rapamycin and tacrolimus concentrations in the blood the day prior to T cell transfer. Graphs show a representative experiment from 3 independent experiments with similar results; Mean \pm SEM from 3–4 mice. RAPA-inj; Rapamycin injection (2mg/kg). TAC-inj; Tacrolimus injection (10mg/kg). (E) Assessment of the effects of drug diets on TCRV α 2⁺ OT-II CD4⁺ T cell proliferation in the inguinal lymph nodes. One experiment, n = 6/group. (A-E) One-way ANOVA with post-hoc Tukey's multiple comparisons test. ns; not significant; OVA: Ovalbumin; BSA: Bovine Serum Albumin.

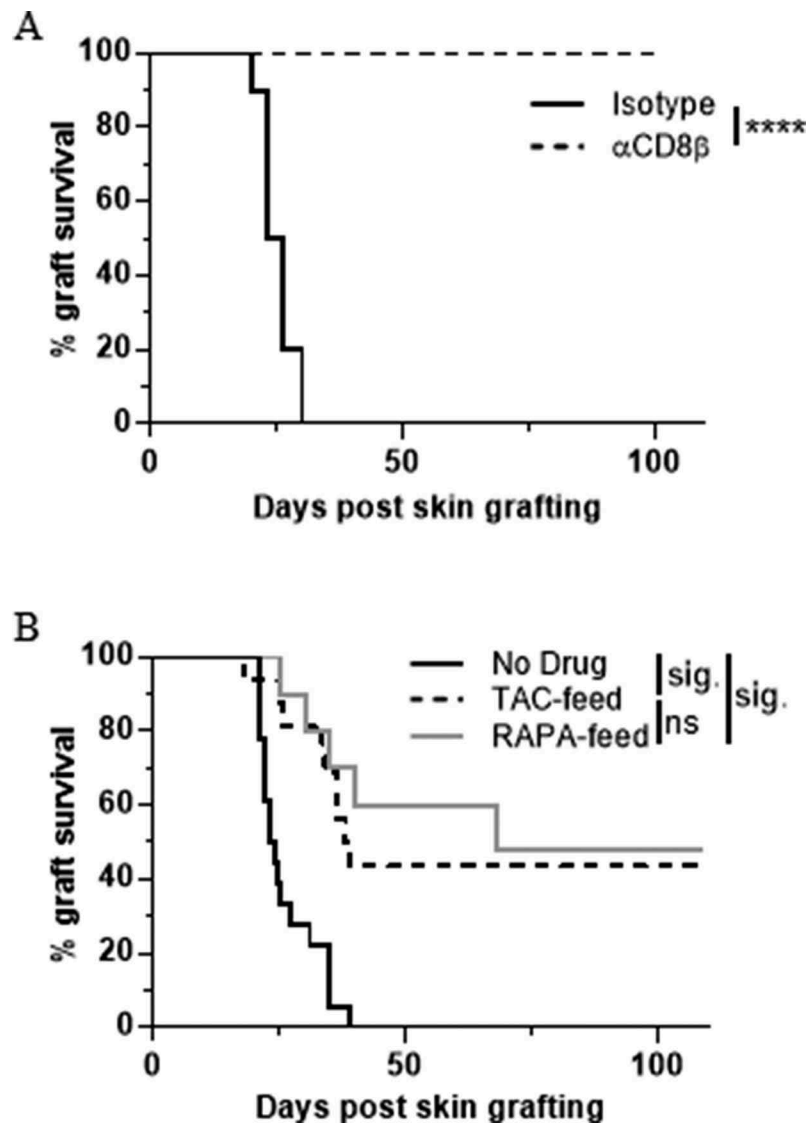


Figure 3. Suppression of CD8⁺ T cell-mediated skin graft rejection. (A) Rejection of K5mOVA-expressing skin grafts is prevented in mice depleted of CD8 T cells. Data shown are combined from 3 independent experiments ($n = 8-10$). Log-rank (Mantel-Cox) test p value = $p < 0.0001$. (B) K5mOVA ear skin graft rejection in C57BL/6 recipient mice pre-treated with rapamycin- or tacrolimus diet for 7–14 days prior to surgery. Treatments were maintained for the duration of the experiment, and skin graft survival monitored. Data shown are combined from 6 independent experiments ($n = 10-18$). Log-rank (Mantel-Cox) test p value = $p < 0.0001$. Results then displayed as significant (sig.) or not significant (ns) after Bonferroni-corrected multiple comparison test. Bonferroni-corrected threshold = 0.016, $K = 3$.

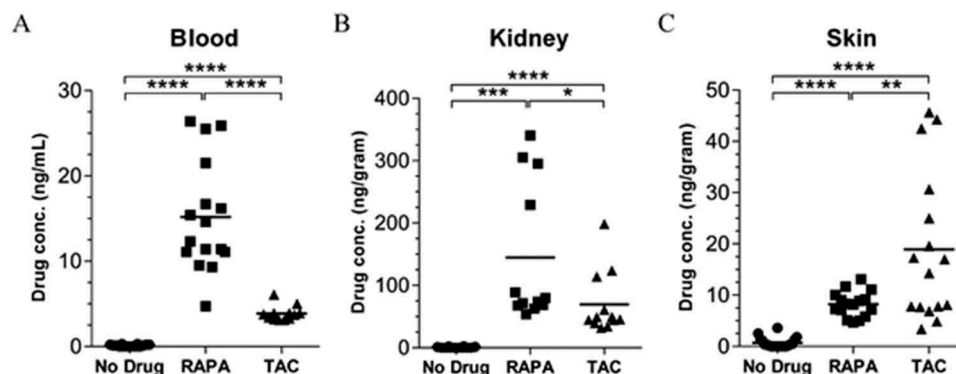


Figure 4. Rapamycin concentration in the skin is low compared to the kidney following the establishment of clinically-relevant blood concentration profiles. C57BL/6 mice were fed with control, rapamycin- or tacrolimus diet for 20 days before harvest of (A) Blood, (B) Kidney, and (C) Skin. Samples were then assayed for drug concentration by LC-MS/MS. Low level drug concentrations seen in the skin of normal diet controls can be attributed to background measurements observed during the HPLC elution process as a consequence of high levels of matrix contaminants. Data shown are combined from 4 independent experiments, $n = 12-20$, bars represent mean. (A-C) One-way ANOVA with post-hoc Tukey's multiple comparisons test. RAPA; Rapamycin diet. TAC; Tacrolimus diet. One data point/animal.

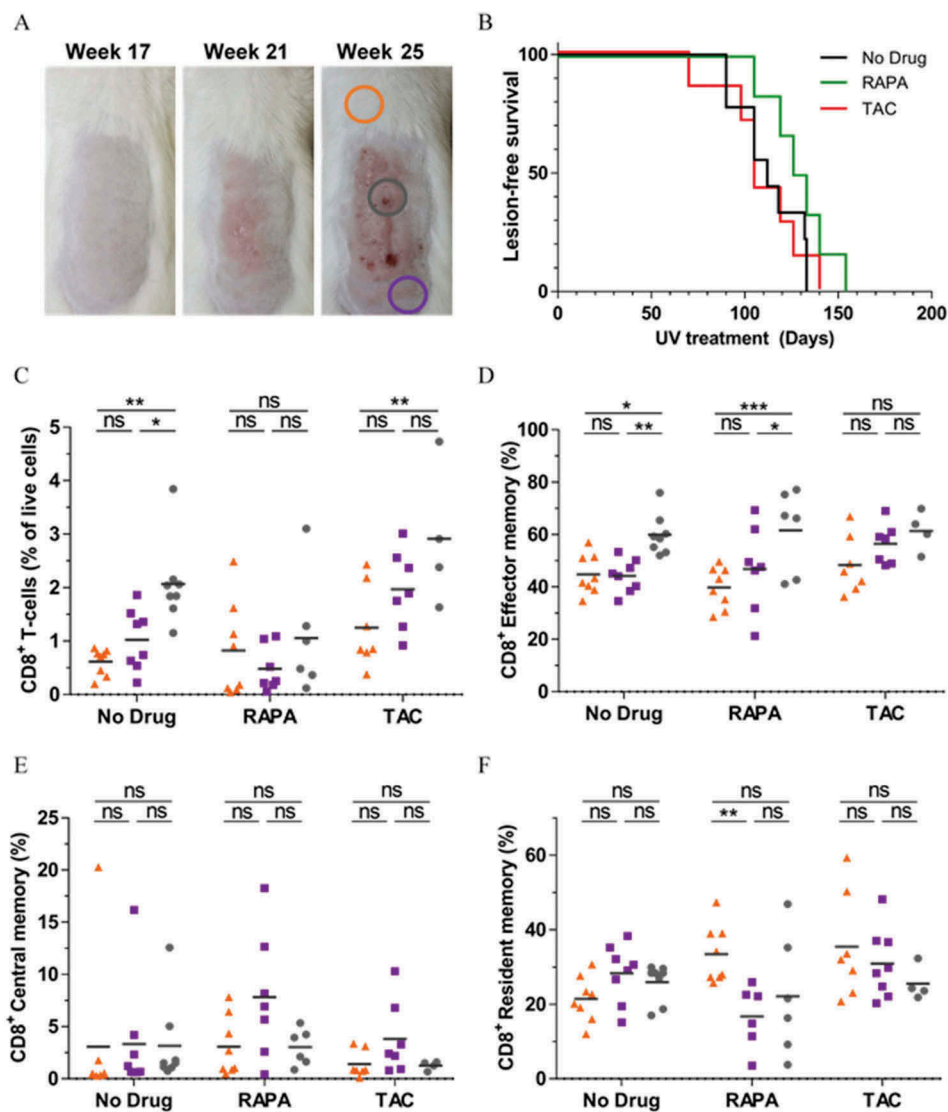


Figure 5. Rapamycin does not prevent the infiltration of effector memory CD8⁺ T cells into AK/SCC lesions. (A) 20+ weeks of UV treatment induces AK/SCC lesion formation in HPV38 E6E7 mice. Colored circles indicate sites of tissue harvest analyzed in (C-F). (B) Rate of AK/SCC lesion formation in mice treated with rapamycin or tacrolimus for the duration UV treatment. (C) CD45⁺CD8⁺ Total, (D) CD45⁺CD8⁺CD69⁺CD103⁻CD44⁺CD62L⁻ Effector Memory, (E) CD45⁺CD8⁺CD69⁺CD103⁻CD44⁺CD62L⁺ Central Memory, and (F) CD45⁺CD8⁺CD69⁺CD103⁺ Resident Memory CD8⁺ T cell abundance in fur-covered (UV-protected) normal skin (orange triangles), UV-exposed non-lesional skin (purple squares) and lesional skin (AK/SCC, grey circles) as indicated in (A). (B) Data pooled from 3 independent experiments, $n = 6-10$, differences not significant (Log-rank (Mantel-Cox) test p value = $p = 0.1770$). (C-F) Data pooled from 3 independent experiments, $n = 4-9$, two-way ANOVA with post-hoc Tukey's multiple comparisons test. One data point/animal.

challenge (Figure 6B; left panel). Differences between drug-treated and non-treated mice were lost following anti-CD8 β antibody treatment however (Figure 6B; right panel), indicating a key role for CD8⁺ T cells in this model.

In a long-term CHS model designed to look at memory CD8⁺ T cell function, drug diets were again commenced on day -15 and maintained throughout the experiment. Mice were sensitized with OVA on day 0, and challenged with OVA in the ear skin on day 45 (Fig. 6Aii). 48 hours after OVA challenge mice treated with rapamycin showed a significantly increased swelling response compared to tacrolimus-treated or non-drug treated mice (Figure 6C; left panel). Interestingly, these responses were still higher following CD8⁺ T cell depletion (Figure 6C; right panel). This enhancement of memory CD8⁺ T cell function would therefore appear to be a beneficial effect of rapamycin. In a similar long-term CHS model,

mice were sensitized with OVA on day 0 and challenged with OVA on day 45, but drug diets were not commenced until day 33 (Figure 6Aiii). In this model the beneficial effects of rapamycin were lost (Figure 6D; left panel, CD8⁺ T cell depletion; right panel), underlying the importance of the presence of rapamycin during OVA sensitization for the enhancement of memory CD8⁺ T cell function.

Quantitation of absolute numbers of effector and central memory CD8⁺ T cells in the ear skin of mice in (Figure 6C) (i.e. drugs given before OVA sensitization) showed that rapamycin treatment, but not tacrolimus treatment, significantly increased both effector and central memory CD8⁺ T cell abundance at the site of OVA challenge (Figures 6E and 6F respectively). Our attempt to measure the antigen-specific production of intracellular IFN- γ and TNF α in these cells was unsuccessful (Supplementary

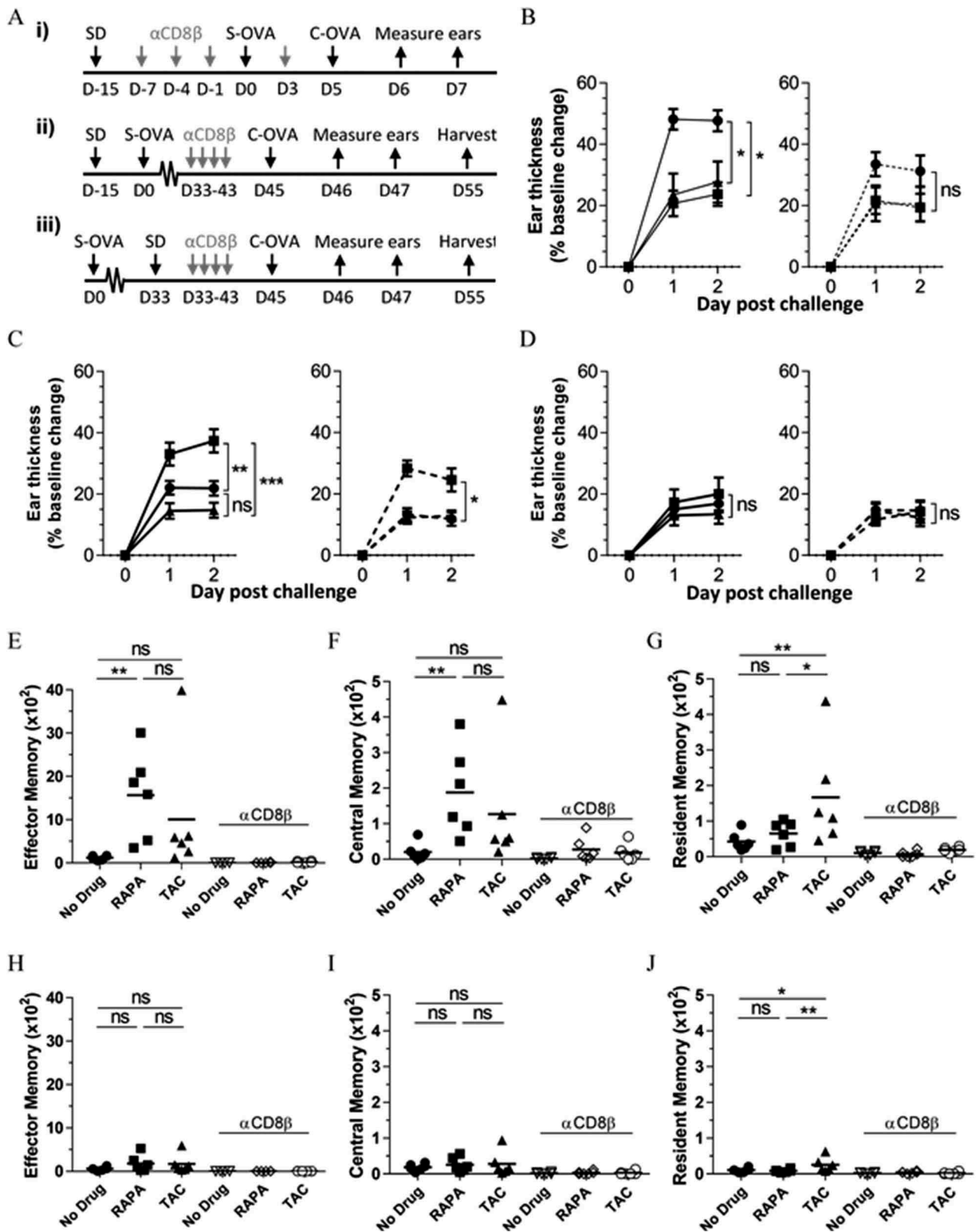


Figure 6. A clinically-relevant rapamycin dose promotes memory CD8⁺ T-cell differentiation and function in response to new antigen-challenges in the skin. (A) Experimental timelines: i) Short-term CHS setup as in B; ii) Memory recall CHS – drugs before sensitisation as in C, E, F, and G; Memory recall CHS – drugs after sensitisation as in D, H, I, and J. (B) Short-term CHS response, (C) Memory CHS response where drug diets are administered 15 days before OVA-sensitisation, and (D) Memory CHS response where drug diets are administered 33 days after OVA-sensitisation. (left panel) Change in ear thickness in OVA-sensitised mice in response to i.d. OVA challenge into the ear skin. (right panel) Effects of systemic CD8⁺ T cell depletion prior to antigen challenge. (B-D) ●; No drug. ■; Rapamycin. ▲; Tacrolimus. Dashed line in right-hand panels = CD8 β depletion. One-way ANOVA with post-hoc Tukey's multiple comparisons test on Day 2 shown. (B) Data are combined from 2 independent experiments, n = 6. (C) and (D) Data are combined from 2 independent experiments, n = 8, mean \pm SEM shown. (E), (F), and (G) Absolute counts of CD45⁺TCR β ⁺CD8 α ⁺CD69⁻CD103⁻ effector memory, CD45⁺TCR β ⁺CD8 α ⁺CD69⁻CD103⁻CD44⁺CD62L⁻ central memory, and CD45⁺TCR β ⁺CD8 α ⁺CD69⁻CD103⁺ resident memory CD8⁺ T cells respectively in the ears of mice on Day 55 as in (C). (H), (I), and (J) Absolute counts of effector memory, central memory, and resident memory CD8⁺ T cells respectively in the ears of mice on Day 55 as in (D). (E-J) CD8 β -depletion groups (open symbols) indicated on graph. (E-G) and (H-J) Data represent one independent experiment from 3 independent experiments with similar results, n = 6, one data point/animal. One-way ANOVA with post-hoc Tukey's multiple comparisons test. ns; not significant. SD: Start Drugs; S-OVA: Sensitisation with OVA; C-OVA: Challenge with OVA; D: Day. Once initiated, mice remained on drug diets for the duration of these experiments.

Figure 3). Conversely, tacrolimus treatment but not rapamycin treatment led to a significant increase in the abundance of resident memory CD8⁺ T cells (Figure 6G). Notably, central memory CD8⁺ T cells were detectable in the ear skin of some rapamycin-treated mice treated with anti-CD8 β antibody (Figure 6F), perhaps explaining the resilience of the ear-thickening response in rapamycin treated mice in Figure 6C.

When absolute numbers of effector and central memory CD8⁺ T cells were quantitated from the ear skin of mice in Figure 6D (i.e. drugs given after OVA sensitization), the effects of rapamycin treatment on increasing effector and central memory CD8⁺ T cell abundance were lost (Figures 6H and 6I respectively). However, the effects of tacrolimus on increasing the abundance of resident memory CD8⁺ T cells were maintained (Figure 6J), suggesting that tacrolimus treatment may increase the abundance of resident memory CD8⁺ T cells in the skin in an antigen-independent manner. Together, these data indicate that clinically-relevant doses of rapamycin present during antigen-sensitization promote memory CD8⁺ T cell function in the skin, with a corresponding increase in the abundance of effector and central, but not resident, memory CD8⁺ T cells at this site.

High dose rapamycin does not promote an increase in central- and effector memory CD8⁺ T cell abundance but does lead to increased CHS recall responsiveness

To define whether the increased swelling response observed in the long-term CHS model following rapamycin treatment (Figure 6C; 6E-G) was the result of the increased absolute numbers of effector and central memory CD8⁺ T cells in the skin, we repeated the experiment outlined in (Figure 6Aii) with the inclusion of the injection of a high dose of rapamycin. As a prelude to this experiment we initially confirmed that the daily i.p. injection of 8mg/kg of rapamycin would lead to an increased concentration of rapamycin in the skin when compared to the levels induced by the rapamycin-diet. We harvested skin after 10 days of rapamycin diet or daily rapamycin injection and analysed the rapamycin concentration by LC-MS/MS. As shown in (Figure 7A), the daily i.p. injection of 8mg/kg of rapamycin corresponded to an approximately 10-fold increase in skin rapamycin concentration. Next, we used the expression of the iron transferrin receptor CD71 on CD8⁺ T-cells in the skin to determine whether the concentrations of rapamycin present in the skin led to a lower a lower inhibition of the mTOR pathway compared with the spleen or inguinal lymph nodes (Figure 7B). Visually, the expression of CD71 appeared higher in the skin than the spleen or lymph nodes, suggesting that indeed the mTOR pathway in CD8⁺ T-cells was more active in the skin than the spleen or lymph nodes, although the differences were not statistically significant. Unexpectedly however, both rapamycin delivery methods appeared not to affect CD71 expression by CD8⁺ T-cells in the skin when compared to control mice (Figure 7B). Since CD71 expression is reported to be up-regulated on activated T cells,⁴⁵ the data suggest that CD8⁺ T-cells might be activate in the skin following both “low dose” (rapamycin-diet) and “high dose” (daily 8mg/kg injection) rapamycin administration.

We repeated the long-term CHS model (as in Figure 6Aii), in which rapamycin was present before antigen sensitisation and maintained throughout the experiment, to determine the

effects of high rapamycin dose treatment. High dose rapamycin treatment, unlike rapamycin-diet, did not increase the absolute numbers of effector and central memory CD8⁺ T cells in the ear skin when compared with the no drug controls (Figures 7C and 7D respectively). Notably, while rapamycin-diet resulted in a significantly greater abundance of effector memory CD8⁺ T cells when compared with high dose rapamycin (Figure 7C), there was not a significant difference in the abundance of central memory CD8⁺ T cells between these two treatments (Figure 7D). Surprisingly, high dose rapamycin treatment induced a similar degree of increased skin swelling in response to antigen challenge as that induced by rapamycin-diet (Figure 7E), suggesting that both drug treatments improved the recall response to OVA. In contrast to rapamycin-diet, however, the surface expression of CD71 on CD8⁺ T cells in the ear skin also increased following high dose rapamycin treatment (Figure 7F). A closer examination of memory marker expression confirmed that this increase was not due to an increase in expression by effector memory CD8⁺ T cells but rather was due to an increase in expression by central memory CD8⁺ T cells (Figures 7G and 7H respectively), suggesting that central memory CD8⁺ T cells were highly activated in the skin of mice receiving high dose rapamycin. Together, these data indicate that high dose rapamycin treatment does not induce the differentiation of effector or central memory CD8⁺ T cells in the skin, but does increase CHS responses. This suggests that the increased CHS responses observed following clinically-relevant doses of rapamycin are not simply a factor of the generation of a greater abundance of effector- or central memory CD8⁺ T cells.

Discussion

The measurement of whole blood concentrations of rapamycin and tacrolimus upon initiation and maintenance of drug therapy is the standard clinical practise in patients with solid organ transplants. The target therapeutic level for these drugs varies depending on individual circumstances; however it is generally considered that an average concentration over a 24-hour period of 10 – 30 ng/ml for rapamycin,⁴² and trough concentration of 5 – 20 ng/ml for tacrolimus⁴³ is needed for effective immunosuppression in the clinic. We have recently confirmed that rapamycin treatment, but not calcineurin inhibitor treatment, leads to significant increases in the abundance of CD8⁺ memory T cells in sun-exposed skin as compared to non-sun exposed skin in kidney transplant patients.²⁷ However, to circumvent the challenges of performing functional assessments of memory CD8⁺ T cells in patient skin, we established drug-incorporated diets, which when fed to mice, resulted in the establishment of clinically-relevant rapamycin and tacrolimus concentrations in the blood. The advantage of this methodology is that mice can be administered drugs orally over long periods of time, as they are in humans, without the need for daily (or twice-daily) injections. The caveat however, is that the level of drugs the mice receive is directly proportional to the amount of food they choose to eat. Nevertheless, despite a slight reduction in overall weight gain (Supplementary Figure 1E), we observed that this method of drug administration was well-tolerated in the mice, and resulted

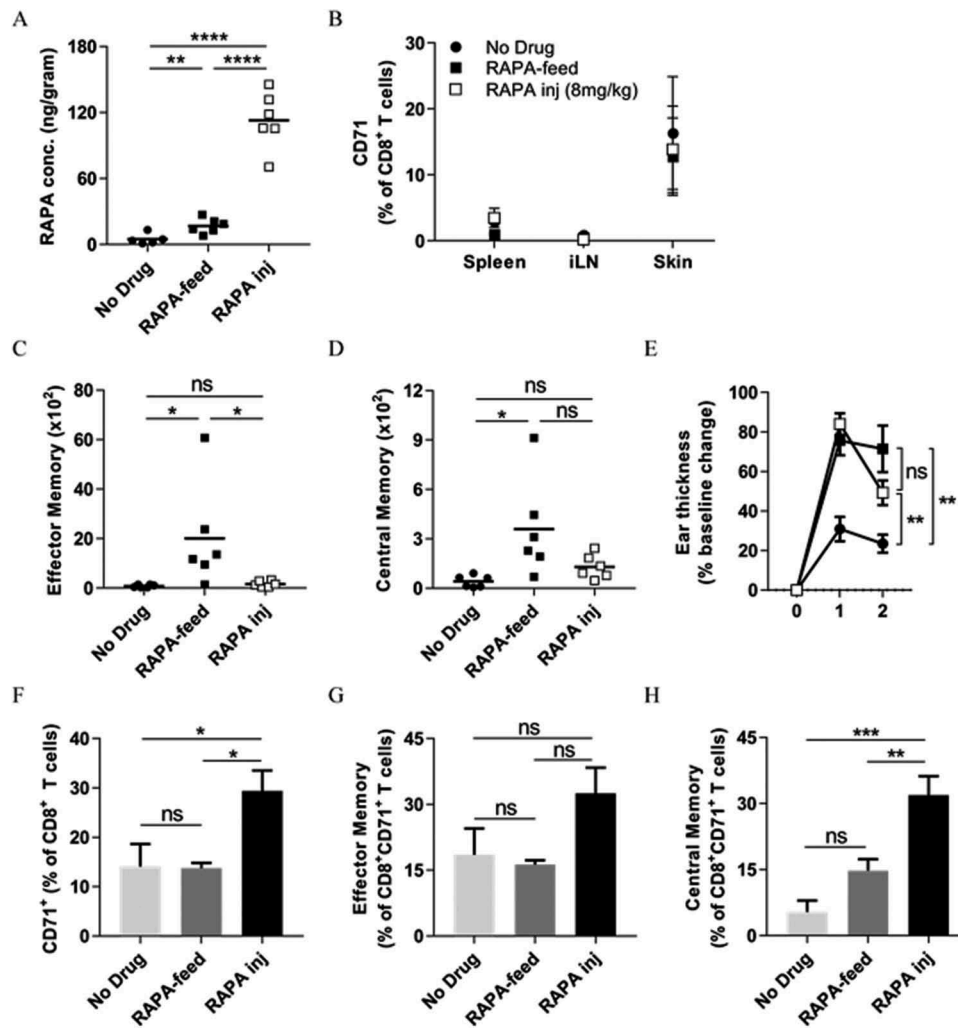


Figure 7. A high rapamycin dose does not promote memory CD8⁺ T-cell differentiation but does enhance long-term CHS responses to OVA. (A-B) C57BL/6 mice were fed with control or rapamycin diet, or injected daily with high dose (8mg/kg) rapamycin for 10 days before tissue harvest. (A) Rapamycin concentration in the skin measured by LC-MS/MS. (B) CD71 surface expression on CD8⁺ T-cells in the spleen, inguinal lymph nodes (iLN), and skin was analysed by FACS. Differences not significant (two-way ANOVA with Dunnett's multiple comparisons test). (C-H) Memory recall CHS – rapamycin before sensitisation as in Fig. 6Aii. C57BL/6 mice were fed with control or rapamycin diet, or injected daily with high dose (8mg/kg) rapamycin throughout the experiment. (C) Absolute counts of CD45⁺TCRβ⁺CD8α⁺CD69⁻CD103⁻CD44⁺CD62L⁻ effector memory, and (D) CD45⁺TCRβ⁺CD8α⁺CD69⁻CD103⁻CD44⁺CD62L⁺ central memory CD8⁺ T cells in the ears of mice on Day 55. (E) Memory CHS response. ●; No drug. ■; Rapamycin diet. □; Daily rapamycin injection (8mg/kg). One-way ANOVA with post-hoc Tukey's multiple comparisons test on Day 2 shown. (F-H) CD71 surface expression on (F) total CD8⁺ T-cells, (G) effector memory CD8⁺ T-cells, and (H) central memory CD8⁺ T-cells in the skin on day 55. (G) and (H), markers as in (C) and (D) respectively. (A), (C), (D), (F-H) One-way ANOVA with post-hoc Tukey's multiple comparisons test. ns; not significant. (A), (C), (D) One data point/animal. Data are derived from one experiment.

in consistent levels of rapamycin being detected in the skin (Figure 4C).

We observed that despite the levels of rapamycin in the blood being higher than for tacrolimus, the accumulation of rapamycin in the skin was much lower. This may explain reports in a previous study describing that the levels of rapamycin needed to delay the rejection of skin allografts are 15–30 fold higher than those needed to completely prevent cardiac allograft rejection. By contrast, equivalent doses of cyclosporine A (belonging to the same class of drugs as tacrolimus) showed a similar efficacy regarding the engraftment of these two tissue types.⁴⁶ Importantly, the levels of rapamycin in the skin (around 8.2 ng per gram on average) appeared to increase the quality and quantity of OVA-specific memory CD8⁺ T cells in the skin in a model of CHS – providing that rapamycin was present during antigen sensitization. This is in keeping with previous reports of

enhancements in the quality and quantity of virus-specific memory CD8⁺ T cells in the lymphoid organs of mice and blood of non-human primates injected i.p. and i.m. (respectively) with rapamycin.²² Thus, our findings may suggest that patients switched to mTOR inhibitor regimens may well benefit from enhanced CD8⁺ memory T cell function to new antigen-challenges in their skin, such as those induced through new UV-induced mutations. We speculated that these beneficial effects in the skin could be lost when the doses of rapamycin that patients receive are too high. Surprisingly, our mouse data suggest that while higher doses of rapamycin may indeed prevent the increases in CD8⁺ memory T cell differentiation seen with lower doses of rapamycin, the improved recall response to OVA in a long-term CHS model was maintained. Furthermore, CD71 expression levels were increased on central memory CD8⁺ T cells in the skin of mice receiving higher doses of rapamycin suggesting

enhanced functionality of these cells. However, the link between the prolonged use of rapamycin, the dose of rapamycin used, and the consequent effects on CD8⁺ T-cell functionality remains poorly-defined, yet warrants further investigation.

Our data further suggest that the effects of rapamycin on “memory” cells in the skin are restricted to effector and central, but not resident, memory subsets. Elsewhere, rapamycin has been reported to inhibit the formation of resident memory CD8⁺ T cells in the intestinal and vaginal mucosa, by inhibiting the formation of resident mucosal memory CD8⁺ T cell precursors.⁴⁷ These findings may be explained, at least in part, by the observation that blockade of the mTOR pathway promotes the expression of the T-box transcription factor eomesodermin,²⁵ but near-extinguishment of eomesodermin is necessary for resident memory T cell development.⁴⁸

We show here that clinically-relevant doses of rapamycin do not appear to impact on the abundance of DC in the epidermis or dermis, at least over the short-term. Similar observations regarding the abundance of Langerhans cells have been made in patient SCC lesions taken before and after conversion from calcineurin inhibitors to sirolimus.⁴⁹ However, a recent study in mice has shown that the homeostasis of Langerhans cells critically depends on mTORC1, which is blocked by rapamycin, and furthermore that the ablation of mTORC1 activity leads to the progressive loss of Langerhans cells in the skin over time due to enhanced migration to the skin draining lymph nodes.⁵⁰ Therefore, future examination of antigen presenting cell types in the skin following the long term use of rapamycin in the context of our- or similar- models appears both timely and appropriate if we are to fully understand the impact of long-term rapamycin use on residual immune function in patient skin.

The impact that rapamycin has on memory T cell differentiation and function within cutaneous SCC lesions in the clinic, and the role that these cells subsequently have in the prevention of *de novo* lesion formation and the regression of premalignant lesions, is currently unclear. In mice however, low dose mTOR inhibition has been shown to produce little interference with the production of effector molecules such as IFN- γ , perforin, or granzyme B.²⁶ Furthermore, the combination of (rapamycin-independent) IFN- γ with rapamycin has recently been shown to promote $\gamma\delta$ TCR^{mid} T cell-mediated prevention of tumour formation in a DMBA/TPA skin carcinogenesis model.⁵¹ The K14 HPV38 E6/E7 mouse model is the only UV-induced mouse tumor model that we are aware of that consistently and specifically produces SCC lesions as oppose to papillomas or mixed skin tumour types. Using this model we show here that unlike tacrolimus-treatment, rapamycin treatment allows the migration of CD8⁺ effector memory T cells into AK/SCC lesions induced by UV-treatment. However, rapamycin-treatment could not prevent lesion formation in UV-treated mice in the first instance. This observation agrees with a previous study utilizing UV-treatment of SKH-1 hairless mice, in which rapamycin reduced the numbers and area of papilloma tumours but could not prevent tumour emergence.⁵² Whether or not rapamycin treatment could allow T cells to prevent SCC emergence is difficult to define

in these models due to the requirement that UV-treatment be used for SCC induction, and the associated immunosuppressive nature of UV-treatment on memory T cell function and development.⁴⁴ Further complicating the issue is the fact that SCC are highly immunogenic tumours,⁵³ and transplantable SCC models often do not establish in immune competent mice.

Taken together, we have demonstrated that unlike clinically-relevant concentrations of tacrolimus in the blood, clinically-relevant concentrations of rapamycin in the blood correspond to a relatively “low dose” drug environment in the skin. This environment allowed the infiltration of CD8⁺ effector memory T cells into UV-induced SCC lesions, and enhanced the number and function of antigen-specific CD8⁺ effector and central memory T cells in the skin following new antigenic challenge. Thus, our findings suggest that patients switched to mTOR inhibitor treatment regimens from calcineurin inhibitor treatment regimens may well benefit from residual CD8⁺ T cell function in their skin. Our results advocate further study into the contribution that immune mechanisms may play in the reduced risk of SCC development associated with rapamycin treatment.

Acknowledgments

We thank the staff at the TRI Flow cytometry core for providing excellent service. The authors declare no conflicts of interest.

Funding

This work was supported by a scholarship to J.J by the Australian Government, a Cancer Council Queensland project grant (APP1128447) to J.W.W and I.H.F, an Australian Research Council Discovery Grant (DP150103714) to J.W.W, R.J.S and I.H.F, an Australian Research Council Future Fellowship (FT110100372) to R.J.S, and a Perpetual Trustees Fellowship to J.W.W.

ORCID

Nana H. Overgaard  <http://orcid.org/0000-0001-6916-9566>

Fiona Simpson  <http://orcid.org/0000-0002-0271-781X>

James W. Wells  <http://orcid.org/0000-0002-9618-6940>

References

1. Jung JW, Overgaard NH, Burke MT, Isbel N, Frazer IH, Simpson F et al. Does the nature of residual immune function explain the differential risk of non-melanoma skin cancer development in immunosuppressed organ transplant recipients?. *International Journal of Cancer*. 2016;138:281–292. doi:10.1002/ijc.29450.
2. Burke MT, Isbel N, Barraclough KA, Jung JW, Wells JW, Staats CE. Genetics and nonmelanoma skin cancer in kidney transplant recipients. *Pharmacogenomics*. 2015;16:161–172. doi:10.2217/pgs.14.156.
3. Ramsay HM, Fryer AA, Hawley CM, Smith AG, Harden PN. Non-melanoma skin cancer risk in the Queensland renal transplant population. *Br J Dermatol*. 2002;147:950–956. doi:10.1046/j.1365-2133.2002.04976.x.
4. Lindelof B, Sigurgeirsson B, Gabel H, Stern RS. Incidence of skin cancer in 5356 patients following organ transplantation. *Br J Dermatol*. 2000;143:513–519.

5. McDonald S, Clayton P, Australia HK, Dialysis NZ, Registry T. 2012. Annual report - 35th Edition. Aust New Zealand Dial Transpl Registry. 2012;48–56. http://www.anzdata.org.au/v1/report_2012.html.
6. Euvrard S, Morelon E, Rostaing L, Goffin E, Brocard A, Tromme I et al. Sirolimus and secondary skin-cancer prevention in kidney transplantation. *N Engl J Med.* 2012;367:329–339. doi:10.1056/NEJMoa1204166.
7. Campbell SB, Walker R, Tai SS, Jiang Q, Russ GR. Randomized controlled trial of sirolimus for renal transplant recipients at high risk for nonmelanoma skin cancer. *Am J Transplantation: Official Journal Am Soc Transplant Am Soc Transpl Surgeons.* 2012;12:1146–1156. doi:10.1111/j.1600-6143.2012.04004.x.
8. Salgo R, Gossmann J, Schofer H, Kachel HG, Kuck J, Geiger H et al. Switch to a sirolimus-based immunosuppression in long-term renal transplant recipients: reduced rate of (pre-)malignancies and nonmelanoma skin cancer in a prospective, randomized, assessor-blinded, controlled clinical trial. *Am J Transplant.* 2010;10:1385–1393. doi:10.1111/j.1600-6143.2009.02997.x.
9. Alberu J, Pascoe MD, Campistol JM, Schena FP, Rial Mdel C, Polinsky M et al. Lower malignancy rates in renal allograft recipients converted to sirolimus-based, calcineurin inhibitor-free immunotherapy: 24-month results from the CONVERT trial. *Transplantation.* 2011;92:303–310. doi:10.1097/TP.0b013e3182247ae2.
10. Yaich S, Charfeddine K, Zaghdane S, El Aoud N, Jarraya F, Kharrat M et al. Sirolimus for the treatment of Kaposi sarcoma after renal transplantation: a series of 10 cases. *Transplant Proc.* 2012;44:2824–2826. doi:10.1016/j.transproceed.2012.09.025.
11. Gutierrez-Dalmau A, Sanchez-Fructoso A, Sanz-Guajardo A, Mazuecos A, Franco A, Rial MC et al. Efficacy of conversion to sirolimus in posttransplantation Kaposi's sarcoma. *Transplant Proc.* 2005;37:3836–3838. doi:10.1016/j.transproceed.2005.10.076.
12. Stallone G, Schena A, Infante B, Di Paolo S, Loverre A, Maggio G et al. Sirolimus for Kaposi's sarcoma in renal-transplant recipients. *N Engl J Med.* 2005;352:1317–1323. doi:10.1056/NEJMoa042831.
13. Hoogendijk-van den Akker JM, Harden PN, Hoitsma AJ, Proby CM, WolterbeekR, Bouwes Bavinck JN et al. Two-year randomized controlled prospective trial converting treatment of stable renal transplant recipients with cutaneous invasive squamous cell carcinomas to sirolimus. *J Clinical Oncology: Official Journal Am Soc Clin Oncol.* 2013;31:1317–1323. doi:10.1200/JCO.2012.45.6376.
14. Kaymakcalan MD, Je Y, Sonpavde G, Galsky M, Nguyen PL, Heng DY et al. Risk of infections in renal cell carcinoma (RCC) and non-RCC patients treated with mammalian target of rapamycin inhibitors. *Br J Cancer.* 2013;108:2478–2484. doi:10.1038/bjc.2013.278.
15. Feldmeyer L, Hofbauer GF, Boni T, French LE, Hafner J. Mammalian target of rapamycin (mTOR) inhibitors slow skin carcinogenesis, but impair wound healing. *Br J Dermatol.* 2012;166:422–424. doi:10.1111/j.1365-2133.2011.10591.x.
16. Russell JJ. Topical tacrolimus: a new therapy for atopic dermatitis. *Am Fam Physician.* 2002;66:1899–1902.
17. Thaci D, Salgo R. Malignancy concerns of topical calcineurin inhibitors for atopic dermatitis: facts and controversies. *Clin Dermatol.* 2010;28:52–56. doi:10.1016/j.clindermatol.2009.04.001.
18. Naylor M, Elmets C, Jaracz E, Rico JM. Non-melanoma skin cancer in patients with atopic dermatitis treated with topical tacrolimus. *J Dermatolog Treat.* 2005;16:149–153. doi:10.1080/09546630510041088.
19. Babel N, Eibl N, Ulrich C, Bold G, Seifrin A, Hammer MH et al. Development of Kaposi's sarcoma under sirolimus-based immunosuppression and successful treatment with imiquimod. *Transpl Infectious Disease: Official Journal Transplant Soc.* 2008;10:59–62. doi:10.1111/j.1399-3062.2007.00239.x.
20. Boratynska M, Zmonarski SC, Klinger M. Recurrence of Kaposi's sarcoma after increased exposure to sirolimus. *Int Immunopharmacol.* 2006;6:2018–2022. doi:10.1016/j.intimp.2006.09.018.
21. Beziaud L, Mansi L, Ravel P, Marie-Joseph EL, Laheurte C, Rangan L et al. Rapalogs Efficacy Relies on the Modulation of Antitumor T-cell Immunity. *Cancer Res.* 2016;76:4100–4112. doi:10.1158/0008-5472.CAN-15-2452.
22. Araki K, Turner AP, Shaffer VO, Gangappa S, Keller SA, Bachmann MF et al. mTOR regulates memory CD8 T-cell differentiation. *Nature.* 2009;460:108–112. doi:10.1038/nature08155.
23. Powell JD, Delgoffe GM. The mammalian target of rapamycin: linking T cell differentiation, function, and metabolism. *Immunity.* 2010;33:301–311. doi:10.1016/j.immuni.2010.09.002.
24. Kaech SM, Cui W. Transcriptional control of effector and memory CD8+ T cell differentiation. *Nat Reviews Immunol.* 2012;12:749–761. doi:10.1038/nri3307.
25. Rao RR, Li Q, Odunsi K, Shrikant PA. The mTOR kinase determines effector versus memory CD8+ T cell fate by regulating the expression of transcription factors T-bet and Eomesodermin. *Immunity.* 2010;32:67–78. doi:10.1016/j.immuni.2009.10.010.
26. Rovira J, Sabet-Baktach M, Eggenhofer E, Lantow M, Koehl GE, Schlitt HJ et al. A color-coded reporter model to study the effect of immunosuppressants on CD8+ T-cell memory in antitumor and alloimmune responses. *Transplantation.* 2013;95:54–62. doi:10.1097/TP.0b013e318276d358.
27. Burke MT, Sambira Nahum LC, Isbel NM, Carroll RP, Soyler HP, Francis R et al. Sirolimus Increases T-Cell Abundance in the Sun Exposed Skin of Kidney Transplant Recipients. *Transplant Direct.* 2017;3:e171. doi:10.1097/TXD.0000000000000694.
28. Callahan MK, Postow MA, Wolchok JD. Targeting T Cell Coreceptors for Cancer Therapy. *Immunity.* 2016;44:1069–1078. doi:10.1016/j.immuni.2016.04.023.
29. Evans CH, Liu F, Porter RM, O'Sullivan RP, Merghoub T, Lunsford EP et al. EWS-FLI-1-targeted cytotoxic T-cell killing of multiple tumor types belonging to the Ewing sarcoma family of tumors. *Clin Cancer Res.* 2012;18:5341–5351. doi:10.1158/1078-0432.CCR-12-1985.
30. Wells JW, Cowled CJ, Darling D, Guinn BA, Farzaneh F, Noble A, et al. Semi-allogeneic dendritic cells can induce antigen-specific T-cell activation, which is not enhanced by concurrent alloreactivity. *Cancer Immunol Immunother.* 2007;56:1861–1873. doi:10.1007/s00262-007-0328-x.
31. Gu T, De Jesus M, Gallagher HC, Burris TP, Egilmez NK. Oral IL-10 suppresses colon carcinogenesis via elimination of pathogenic CD4(+) T-cells and induction of antitumor CD8(+) T-cell activity. *Oncoimmunology.* 2017;6:e1319027. doi:10.1080/2162402X.2017.1319027.
32. Kilinc MO, Gu T, Harden JL, Virtuoso LP, Egilmez NK. Central role of tumor-associated CD8+ T effector/memory cells in restoring systemic antitumor immunity. *J Immunol.* 2009;182:4217–4225. doi:10.4049/jimmunol.0802793.
33. Lim WA, June CH. The Principles of Engineering Immune Cells to Treat Cancer. *Cell.* 2017;168:724–740. doi:10.1016/j.cell.2017.01.016.
34. Wells JW, Cowled CJ, Giorgini A, Kemeny DM, Noble A. Regulation of allergic airway inflammation by class I-restricted allergen presentation and CD8 T-cell infiltration. *J Allergy Clin Immunol.* 2007;119:226–234. doi:10.1016/j.jaci.2006.09.004.
35. Wells JW, Choy K, Lloyd CM, Noble A. Suppression of allergic airway inflammation and IgE responses by a class I restricted allergen peptide vaccine. *Mucosal Immunology.* 2009;2:54–62. doi:10.1038/mi.2008.69.
36. Freeman A, Bridge JA, Maruthayanar P, Overgaard NH, Jung JW, Simpson F et al. Comparative immune phenotypic analysis of cutaneous Squamous Cell Carcinoma and Intraepidermal Carcinoma in immune-competent individuals: proportional representation of CD8+ T-cells but not FoxP3+ Regulatory T-cells is associated with disease stage. *PLoS One.* 2014;9:e110928. doi:10.1371/journal.pone.0110928.
37. Azukizawa H, Kosaka H, Sano S, Heath WR, Takahashi I, Gao XH et al. Induction of T-cell-mediated skin disease specific for antigen transgenically expressed in keratinocytes. *Eur J Immunol.* 2003;33:1879–1888. doi:10.1002/eji.200323630.
38. Viarisis D, Mueller-Decker K, Kloz U, Aengeneyndt B, Kopp-Schneider A, Grone HJ et al. E6 and E7 from beta HPV38 cooperate with ultraviolet light in the development of actinic keratosis-like lesions and squamous cell carcinoma in mice. *PLoS Pathog.* 2011;7:e1002125. doi:10.1371/journal.ppat.1002125.

39. Wells JW, Darling D, Farzaneh F, Galea-Lauri J. Influence of interleukin-4 on the phenotype and function of bone marrow-derived murine dendritic cells generated under serum-free conditions. *Scand J Immunol.* 2005;61:251–259. doi:10.1111/sji.2005.61.issue-3.
40. Wells JW, Cowled CJ, Farzaneh F, Noble A. Combined triggering of dendritic cell receptors results in synergistic activation and potent cytotoxic immunity. *Journal of Immunology.* 2008;181:3422–3431. doi:10.4049/jimmunol.181.5.3422.
41. Diener KR, Moldenhauer LM, Lyons AB, Brown MP, Hayball JD. Human Flt-3-ligand-mobilized dendritic cells require additional activation to drive effective immune responses. *Exp Hematol.* 2008;36:51–60. doi:10.1016/j.exphem.2007.08.024.
42. Napoli KL, Kahan BD. Routine clinical monitoring of sirolimus (rapamycin) whole-blood concentrations by HPLC with ultraviolet detection. *Clin Chem.* 1996;42:1943–1948.
43. Bottiger Y, Brattstrom C, Tyden G, Sawe J, Groth CG. Tacrolimus whole blood concentrations correlate closely to side-effects in renal transplant recipients. *Br J Clin Pharmacol.* 1999;48:445–448. doi:10.1046/j.1365-2125.1999.00007.x.
44. Rana S, Byrne SN, MacDonald LJ, Chan CY, Halliday GM. Ultraviolet B suppresses immunity by inhibiting effector and memory T cells. *Am J Pathol.* 2008;172:993–1004. doi:10.2353/ajpath.2008.070517.
45. Zheng Y, Collins SL, Lutz MA, Allen AN, Kole TP, Zarek PE et al. A role for mammalian target of rapamycin in regulating T cell activation versus anergy. *J Immunol.* 2007;178:2163–2170. doi:10.4049/jimmunol.178.4.2163.
46. Li Y, Li XC, Zheng XX, Wells AD, Turka LA, Strom TB. Blocking both signal 1 and signal 2 of T-cell activation prevents apoptosis of alloreactive T cells and induction of peripheral allograft tolerance. *Nat Med.* 1999;5:1298–1302. doi:10.1038/15256.
47. Sowell RT, Rogozinska M, Nelson CE, Vezys V, Marzo AL. Cutting edge: generation of effector cells that localize to mucosal tissues and form resident memory CD8 T cells is controlled by mTOR. *J Immunol.* 2014;193:2067–2071. doi:10.4049/jimmunol.1400074.
48. Mackay LK, Wynne-Jones E, Freestone D, Pellicci DG, Mielke LA, Newman DM et al. T-box Transcription Factors Combine with the Cytokines TGF-beta and IL-15 to Control Tissue-Resident Memory T Cell Fate. *Immunity.* 2015;43:1101–1111. doi:10.1016/j.immuni.2015.11.008.
49. Rival-Tringali AL, Euvrard S, Decullier E, Claudy A, Faure M, Kanitakis J. Conversion from calcineurin inhibitors to sirolimus reduces vascularization and thickness of post-transplant cutaneous squamous cell carcinomas. *Anticancer Res.* 2009;29:1927–1932.
50. Kellersch B, Brocker T. Langerhans cell homeostasis in mice is dependent on mTORC1 but not mTORC2 function. *Blood.* 2013;121:298–307. doi:10.1182/blood-2012-06-439786.
51. Dao V, Liu Y, Pandeswara S, Svatek RS, Gelfond JA, Liu A et al. Immune-Stimulatory Effects of Rapamycin Are Mediated by Stimulation of Antitumor gammadelta T Cells. *Cancer Res.* 2016;76:5970–5982. doi:10.1158/0008-5472.CAN-16-0091.
52. Wulff BC, Kusewitt DF, VanBuskirk AM, Thomas-Ahner JM, Duncan FJ, Oberyzyzn TM. Sirolimus reduces the incidence and progression of UVB-induced skin cancer in SKH mice even with co-administration of cyclosporine A. *J Invest Dermatol.* 2008;128:2467–2473. doi:10.1038/jid.2008.121.
53. Kripke ML. Antigenicity of murine skin tumors induced by ultraviolet light. *J Natl Cancer Inst.* 1974;53:1333–1336. doi:10.1093/jnci/53.5.1333.